AIAA JOURNAL
Vol. 42, No. 9, September 2004

Pressure History at the Thrust Wall of a Simplified Pulse Detonation Engine

Takuma Endo*
Hiroshima University, Hiroshima 739-8527, Japan
Jiro Kasahara†
University of Tsukuba, Ibaraki 305-8573, Japan
Akiko Matsuo,‡ Kazuaki Inaba,§ and Shigeru Sato§
Keio University, Kanagawa 223-8522, Japan
and
Toshi Fujiwara¶
ATES Corporation, Aichi 471-0845, Japan

Gas dynamics in a simplified pulse detonation engine (PDE) was theoretically analyzed. A PDE was simplified as a straight tube with a fixed cross section. One end of the tube was closed, namely, this end was the thrust wall, and the other end was open. A detonation wave was initiated at the closed end and simultaneously started to propagate toward the open end. When the detonation wave broke out from the open end, a rarefaction wave started to propagate from the open end toward the closed end. This rarefaction wave was reflected by the closed end. By considering this rarefaction wave to be self-similar in the analysis of the interference between this rarefaction wave and its reflection from the closed end, we analytically formulated the decay portion of the pressure history at the closed end (thrust wall) without any empirical parameters. By integrating the obtained pressure history at the thrust wall with respect to time, important performance parameters of a PDE were also formulated. The obtained formulas were compared with numerical and experimental results and agreed with them very well.

Nomenclature

a	=	sound speed
D_{CJ}	=	Chapman–Jouguet detonation speed
F_n, $F_{n'}$	=	function describing I_{cyc} for n or n'
f_n, $f_{n'}$	=	function describing thrust-decay history for n or n'
g	=	standard sea-level value of gravitational acceleration
I_{cyc}	=	impulse per unit cross section per one cycle
$I_{\mathrm{cyc(+)}}$	=	impulse per unit cross section per one cycle contributed by positive overpressure
I_{sp}	=	mixture-based specific impulse
$I_{\mathrm{sp(+)}}$	=	mixture-based specific impulse contributed by positive overpressure
I_{spf}	=	fuel-based specific impulse
$I_{\mathrm{spf(+)}}$	=	fuel-based specific impulse contributed by positive overpressure
K	=	empirical parameter used in semi-empirical formula proposed in Refs. 4 and 8
k_A	=	numerical constant
k_B	=	numerical constant
k_C	=	numerical constant
L	=	length of pulse detonation engine (PDE) tube
M_{CJ}	=	propagation Mach number of Chapman–Jouguet detonation wave; $M_{\mathrm{CJ}} = D_{\mathrm{CJ}}/a_1$
n	=	positive integer which relates to γ_2 as $\gamma_2 = (2n+3)/(2n+1)$
n'	=	parameter used in calculating approximate thrust-decay history for arbitrary γ_2
n_a, n_b	=	positive integers (1, 2, 3, 4, 6, or 10) used in calculating approximate thrust-decay history for arbitrary γ_2
p	=	pressure
r	=	radius of PDE tube
T	=	temperature
t	=	time relative to the instant of ignition
t^*	=	time at which $x_{\mathrm{rf}} = x_3$
$t^{\#}$	=	time at which $x_{\mathrm{ir}} = L$
t_{CJ}	=	time at which detonation wave reaches open end of PDE tube
t_{exhaust}	=	time at which $p_w = p_1$
t_{plateau}	=	time at which plateau in pressure history at thrust wall ends
t_{valid}	=	time until which obtained thrust-decay history is valid
t'_{valid}	=	time defined by $L = \int_{t^{\#}}^{t'_{\mathrm{valid}}} a_w \, \mathrm{d}t$
u	=	flow velocity in x coordinate
X	=	parameter used in calculating approximate thrust-decay history for arbitrary γ_2
x	=	coordinate along axis of PDE tube, where $x = 0$ and $x = L$ correspond to closed and open ends, respectively
x_{ir}	=	boundary of interference region between exhausting rarefaction wave and its reflection from closed end of PDE tube
x_{rf}	=	front boundary of exhausting rarefaction wave
x^*_{rf}	=	x_{rf} at the time t^*
γ	=	specific-heat ratio

Received 3 March 2003; revision received 28 February 2004; accepted for publication 5 April 2004.

*Associate Professor, Department of Mechanical Engineering, 1-4-1 Kagamiyama, Higashi-Hiroshima; takuma@mec.hiroshima-u.ac.jp. Member AIAA.
†Assistant Professor, Institute of Engineering Mechanics and Systems, 1-1-1 Tennodai, Tsukuba. Member AIAA.
‡Associate Professor, Department of Mechanical Engineering, Hiyoshi 3-14-1, Kohoku-ku, Yokohama. Member AIAA.
§Graduate Student, School of Science for Open and Environmental Systems, Hiyoshi 3-14-1, Kohoku-ku, Yokohama. Student Member AIAA.
¶Technical Adviser, Tanaka-cho 1-118-3, Toyota. Member AIAA.

γ_a, γ_b = parameter used in calculating approximate thrust-decay history for arbitrary γ_2
Δp = instantaneous thrust per unit cross section
δ_{A1} = constant determined by γ_1, γ_2, and M_{CJ}
δ_{A2} = constant determined by γ_1, γ_2, and M_{CJ}
δ_B = constant determined by γ_1, γ_2, and M_{CJ}
ρ = mass density
τ = period of one cycle of PDE operation
ϕ_f = mass fraction of fuel in initial detonable gas mixture

Subscripts

out = outer surface of thrust wall of PDE tube
w = inner surface of thrust wall of PDE tube
1 = undisturbed region ahead of detonation wave
2 = rear surface of detonation wave
3 = rear boundary of decelerating rarefaction wave

Introduction

A PULSE detonation engine (PDE) is an internal combustion engine in which fuel is repetitively burned as self-sustained detonation waves.[1,2] Because a PDE is of simpler structure and of higher theoretical thermal efficiency compared with a conventional internal combustion engine based on isobaric combustion, research and development for its practical applications are underway throughout the world.

Most of experimental studies on PDEs have been carried out by using simplified PDEs.[3–7] Here we call a straight detonation tube with fixed cross section, one end of which is closed and the other end open, a simplified PDE. Against the background of such experimental studies, modeling studies to predict PDE performances have been progressed mainly on simplified PDEs. As such models, semi-empirical models including an empirical parameter, which should be determined by comparison between the semi-empirical formula and experimental results, were proposed.[4,8] And although the authors proposed an analytical model[9] including no empirical parameter, the model was usable only for qualitative prediction of PDE performances because a rarefaction wave, through which the burned gas was exhausted, was not correctly treated.

In this paper, we present analytical formulation, without any empirical parameters, of pressure history at the thrust wall of a simplified PDE. Especially important progress in this work is the formulation of the decay portion of the pressure history at the thrust wall. Only after this formulation, one can predict the time at which overpressure at the thrust wall turns negative from positive. This time is a key parameter when determining the time sequence of the valves of a PDE.

In the following, we explain the setup of the problem first. After that, we describe an overview of gas dynamics in a simplified PDE. Next, details of the formulation of the pressure history at the thrust wall are presented. Performance parameters of a simplified PDE are also formulated by integrating the pressure history at the thrust wall with respect to time. After completing the formulation, we discuss the applicability and validity of the obtained formulas by comparing them with numerical and experimental results. We summarize the principal results in the final section.

Setup of the Problem

A PDE is simplified as a straight tube with fixed cross section as shown in Fig. 1. One end of the tube is closed, namely, this end is the thrust wall, and the other end is open. The instantaneous thrust per unit cross section is written as

$$\Delta p = p_w - p_{\text{out}} \tag{1}$$

The tube is initially filled with uniform detonable gas at rest. A detonation wave is initiated at the time $t = 0$ and at the location $x = 0$. Because of the explosive combustion of the detonable gas, p_w increases. Figure 2 schematically shows the pressure history at the thrust wall. The burned gas is exhausted through the open end of the tube, and thereby p_w decreases gradually. The pressure p_w decreases to the initial value at the time t_{exhaust}. After the time t_{exhaust}, purge of the residual burned gas and recharge of the fresh unburned gas are carried out.

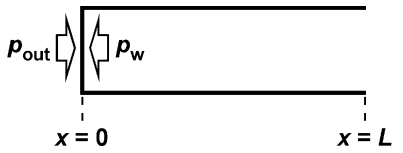

Fig. 1 Simplified PDE.

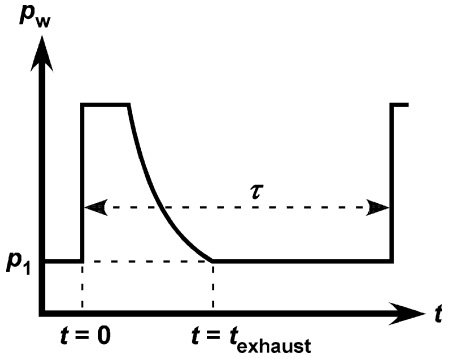

Fig. 2 Schematic of the pressure history at the thrust wall.

The impulse per unit cross section per one cycle of a simplified PDE is written as

$$I_{\text{cyc}} = \int_0^{\tau} \Delta p \, \mathrm{d}t = \int_0^{t_{\text{exhaust}}} (p_w - p_1) \, \mathrm{d}t + (p_1 - p_{\text{out}})\tau \tag{2}$$

In the preceding formula, it was assumed for simplicity that the purge of the residual burned gas and the recharge of the fresh unburned gas are carried out under the pressure p_1, and that variation of p_{out} during τ is negligible.

In the following, all gas dynamics but the detonation wave will be treated as isentropic processes. The thickness of the detonation wave will be neglected. The effects of viscosity and thermal conduction will be also neglected. Furthermore, all gas dynamics in the tube will be treated as one-dimensional.

Overview of the Gas Dynamics in the Tube

Figure 3 shows a schematic space–time (x–t) diagram of characteristics in the tube. We describe an overview of the gas dynamics in one cycle of PDE operation next.

The tube is initially filled with uniform detonable gas at rest. The initial undisturbed gas is characterized by γ_1, p_1, a_1, and $u_1(=0)$. At the time $t = 0$, a detonation wave is initiated at the closed end ($x = 0$) and simultaneously starts to propagate toward the open end. The burned gas at the rear surface of the detonation wave is characterized by γ_2, p_2, a_2, and u_2. In Fig. 3, x_2 denotes the position of the detonation wave.

Because a detonation wave is a compression wave, the gas at the rear surface of the detonation wave has a finite velocity, which is in the same direction as the propagation of the detonation wave, that is, $u_2 > 0$. Because the gas at the closed end has to be at rest, the burned gas is decelerated to $u = 0$ between the detonation wave and the closed end. Because this decelerating flow is characterized by a characteristic speed, that is, sound speed, but by no characteristic length, this deceleration should be realized by a self-similar rarefaction wave following the detonation wave.[10] We call this rarefaction wave the decelerating rarefaction wave hereafter. (This rarefaction wave is often called the Taylor wave.) For the detonation wave to be stable, it must be a Chapman–Jouguet (CJ) detonation wave[11] because it is followed by the decelerating rarefaction wave. The front boundary of the decelerating rarefaction wave coincides with the rear surface of the CJ detonation wave. The gas at the rear boundary of the decelerating rarefaction wave is characterized by $\gamma_3(=\gamma_2)$, p_3, a_3, and $u_3(=0)$. The rear boundary of the decelerating rarefaction wave also propagates toward the open end, whose position is

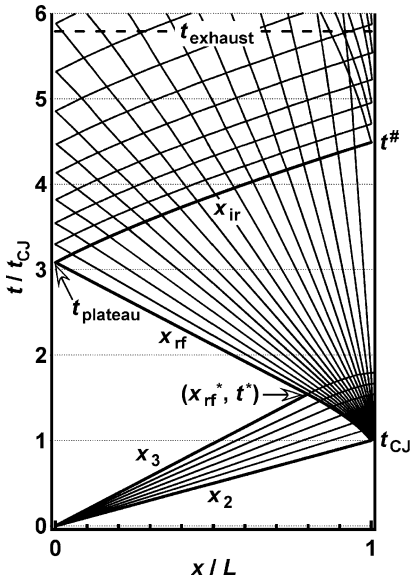

Fig. 3 Schematic space–time (x–t) diagram of characteristics in a simplified PDE.

denoted by x_3 in Fig. 3. Also all gas in the region $0 \le x \le x_3$ is characterized by $\gamma_3(=\gamma_2)$, p_3, a_3, and $u_3(=0)$. The detonation wave reaches the open end at the time t_{CJ}.

The detonation wave is transmitted to the outside of the tube as an inert shock wave, which rapidly decays due to the three-dimensional divergence effect. And the gas flow inside the decelerating rarefaction wave is subsonic. Therefore, another rarefaction wave starts to propagate from the open end toward the closed end at the time t_{CJ}. Through this rarefaction wave, the burned gas is exhausted from the open end. We call this rarefaction wave the exhausting rarefaction wave hereafter. Although this rarefaction wave might be initially preceded by a reflected shock wave in some cases depending on the initial conditions,[8] the preceding shock wave can be rapidly attenuated by the following rarefaction wave because the rarefaction front travels faster than the preceding shock wave. Accordingly, we ignore the preceding shock wave for simplicity. The position of the front boundary of the exhausting rarefaction wave is denoted by x_{rf} in Fig. 3. The front boundary of the exhausting rarefaction wave initially propagates in the decelerating rarefaction wave and intersects the rear boundary of the decelerating rarefaction wave at the time t^* and at the location x_{rf}^*, and after that, propagates to the closed end in the uniform gas at rest characterized by $\gamma_3(=\gamma_2)$, p_3, a_3, and $u_3(=0)$. The front boundary of the exhausting rarefaction wave reaches the closed end at the time $t_{plateau}$. In the time region $0 < t \le t_{plateau}$ (the time $t = 0$ is singular in this analysis), the pressure at the closed end is kept to be $p_w = p_3$. That is, the pressure history at the thrust wall shows a plateau.

After the time $t_{plateau}$, the pressure at the thrust wall decays in the manner determined by interference between the exhausting rarefaction wave and its reflection from the thrust wall. Their interference region extends from the closed end toward the open end, the boundary of which is denoted by x_{ir} in Fig. 3 and reaches the open end at the time $t^{\#}$. At the time $t_{exhaust}$, the pressure at the thrust wall decreases to the initial pressure, and the purge of the residual burned gas is started for the next cycle.

Analysis and Formulation

Plateau in the Thrust History

Parameters describing the state of the burned gas at the rear surface of the detonation wave are given by

$$p_2 = \frac{\gamma_1 M_{CJ}^2 + 1}{\gamma_2 + 1} p_1 \tag{3a}$$

$$a_2 = \frac{\gamma_1 M_{CJ}^2 + 1}{\gamma_1 M_{CJ}^2} \frac{\gamma_2}{\gamma_2 + 1} D_{CJ} \tag{3b}$$

$$u_2 = \frac{\gamma_1 M_{CJ}^2 - \gamma_2}{\gamma_1 M_{CJ}^2} \frac{1}{\gamma_2 + 1} D_{CJ} \tag{3c}$$

These formulas were obtained by using the results in Ref. 11. And by neglecting the thickness of the detonation wave, the position of the rear surface of the detonation wave is given by

$$x_2 = D_{CJ} t \tag{3d}$$

Additionally, the detonation wave reaches the open end at the time

$$t_{CJ} = L / D_{CJ} \tag{4}$$

The time t_{CJ} is a characteristic time of the gas dynamics in the tube.

The state of the gas inside the decelerating rarefaction wave, namely, in the spatial region $x_3 < x < x_2$, is given by

$$p = \left(1 - \frac{\gamma_2 - 1}{\gamma_2 + 1} \frac{x_2 - x}{a_2 t}\right)^{2\gamma_2/(\gamma_2 - 1)} \frac{\gamma_1 M_{CJ}^2 + 1}{\gamma_2 + 1} p_1 \tag{5a}$$

$$a = \frac{\gamma_1 M_{CJ}^2 + \gamma_2}{\gamma_1 M_{CJ}^2} \frac{1}{\gamma_2 + 1} D_{CJ} + \frac{\gamma_2 - 1}{\gamma_2 + 1} \frac{x}{t} \tag{5b}$$

$$u = -\frac{\gamma_1 M_{CJ}^2 + \gamma_2}{\gamma_1 M_{CJ}^2} \frac{1}{\gamma_2 + 1} D_{CJ} + \frac{2}{\gamma_2 + 1} \frac{x}{t} (< a) \tag{5c}$$

These formulas were obtained by using the results in Ref. 12 and the boundary condition that the front boundary of the decelerating rarefaction wave coincides with the rear surface of the CJ detonation wave. The inequality $u < a$ was derived by using the inequalities $x \le x_2$ and $1 < \gamma_2$. Further, the state of the gas at the rear boundary of the decelerating rarefaction wave, which is also the state of the gas occupying the region $0 \le x \le x_3$, is given by

$$p_3 = \delta_{A1} p_1 \tag{6a}$$

$$a_3 = D_{CJ} / \delta_{A2} \tag{6b}$$

$$x_3 = a_3 t \tag{6c}$$

where

$$\delta_{A1} = \frac{\gamma_1 M_{CJ}^2 + \gamma_2}{2\gamma_2} \left(\frac{\gamma_1 M_{CJ}^2 + \gamma_2}{\gamma_1 M_{CJ}^2 + 1} \frac{\gamma_2 + 1}{2\gamma_2}\right)^{(\gamma_2 + 1)/(\gamma_2 - 1)} \tag{7a}$$

$$\delta_{A2} = 2 \frac{\gamma_1 M_{CJ}^2}{\gamma_1 M_{CJ}^2 + \gamma_2} \tag{7b}$$

These formulas were obtained by using the formulas (5a–5c) and the boundary condition that $u_3 = 0$. The pressure p_3 is the plateau pressure in the thrust history, which is one of the important parameters characterizing performances of a PDE. When $M_{CJ}^2 \gg 1$, δ_{A1} and δ_{A2} would become, respectively,

$$\delta_{A1}|_{M_{CJ}^2 \gg 1} \approx (\gamma_1/\gamma_2) \tfrac{1}{2} M_{CJ}^2 [(\gamma_2 + 1)/2\gamma_2]^{(\gamma_2 + 1)/(\gamma_2 - 1)} \tag{8a}$$

$$\delta_{A2}|_{M_{CJ}^2 \gg 1} \approx 2 \tag{8b}$$

We adopted the two-γ model. If the one-γ model were adopted, the plateau pressure in the thrust history would be given by

$$p_3|_{\gamma_1 = \gamma_2 = \gamma} = \frac{M_{CJ}^2 + 1}{2} \left(\frac{M_{CJ}^2 + 1}{\gamma M_{CJ}^2 + 1} \frac{\gamma + 1}{2}\right)^{(\gamma + 1)/(\gamma - 1)} p_1 \tag{9a}$$

This result was derived in Ref. 8. Further, when $M_{CJ}^2 \gg 1$, this would become

$$p_3|_{\gamma_1 = \gamma_2 = \gamma, M_{CJ}^2 \gg 1} \approx \tfrac{1}{2} M_{CJ}^2 [(\gamma + 1)/2\gamma]^{(\gamma + 1)/(\gamma - 1)} p_1 \tag{9b}$$

This result was derived in Ref. 4. The formulas (6a), (8a), and (9b) show that the one-γ model would bring the plateau pressure in the

thrust history lower by a factor of γ_2/γ_1 than the two-γ model when $M_{CJ}^2 \gg 1$, which is almost satisfied in most laboratory experiments. Because the factor γ_2/γ_1 is not so close to unity in general, the two-γ model is more suitable in the formulation of PDE performances.

The exhausting rarefaction wave starts to propagate from the open end toward the closed end (thrust wall) at the time t_{CJ}. The front boundary of the exhausting rarefaction wave is the leading characteristic that starts to propagate from the open end toward the closed end at the time t_{CJ}. This characteristic initially propagates in the decelerating rarefaction wave. Because the sound speed and the flow velocity in the decelerating rarefaction wave were given by Eqs. (5b) and (5c), respectively, the propagation velocity of this characteristic is written as

$$\frac{dx_{rf}}{dt} = u - a = -\frac{\gamma_1 M_{CJ}^2 + \gamma_2}{\gamma_1 M_{CJ}^2}\frac{2}{\gamma_2 + 1} D_{CJ} + \frac{3 - \gamma_2}{\gamma_2 + 1}\frac{x_{rf}}{t} (<0) \quad (10)$$

By solving this differential equation with the condition that $x_{rf} = L$ when $t = t_{CJ}$, the following solution is obtained:

$$x_{rf} = \frac{D_{CJ} t}{\gamma_2 - 1}\left[\gamma_2 \frac{\gamma_1 M_{CJ}^2 + 1}{\gamma_1 M_{CJ}^2}\left(\frac{t_{CJ}}{t}\right)^{2(\gamma_2 - 1)/(\gamma_2 + 1)} - \frac{\gamma_1 M_{CJ}^2 + \gamma_2}{\gamma_1 M_{CJ}^2}\right] \quad (11)$$

This solution is valid only when $x_3 \le x_{rf}$. This characteristic intersects the rear boundary of the decelerating rarefaction wave at the time t^* and at the location x_{rf}^*. The time t^* and the location x_{rf}^* are obtained by using Eq. (11) and the condition that $x_{rf} = x_3$ as follows:

$$t^* = \left(\frac{\gamma_1 M_{CJ}^2 + \gamma_2}{\gamma_1 M_{CJ}^2 + 1}\frac{\gamma_2 + 1}{2\gamma_2}\right)^{-(\gamma_2 + 1)/2(\gamma_2 - 1)} t_{CJ} \quad (12a)$$

$$x_{rf}^* = \frac{1}{\delta_{A2}}\left(\frac{\gamma_1 M_{CJ}^2 + \gamma_2}{\gamma_1 M_{CJ}^2 + 1}\frac{\gamma_2 + 1}{2\gamma_2}\right)^{-(\gamma_2 + 1)/2(\gamma_2 - 1)} L \quad (12b)$$

After the time t^*, the front boundary of the exhausting rarefaction wave propagates toward the closed end with the sound speed a_3 because the gas in the region $0 \le x \le x_3$ is at rest. Therefore, the front boundary of the exhausting rarefaction wave reaches the closed end at the time $t_{plateau}$, which is given by

$$t_{plateau} = t^* + x_{rf}^*/a_3 = \delta_B t_{CJ} \quad (13)$$

where

$$\delta_B = 2\left(\frac{\gamma_1 M_{CJ}^2 + \gamma_2}{\gamma_1 M_{CJ}^2 + 1}\frac{\gamma_2 + 1}{2\gamma_2}\right)^{-(\gamma_2 + 1)/2(\gamma_2 - 1)} \quad (14)$$

In the time region $0 < t \le t_{plateau}$, the pressure at the closed end (thrust wall) is kept to be $p_w = p_3$. When $M_{CJ}^2 \gg 1$, δ_B would become

$$\delta_B|_{M_{CJ}^2 \gg 1} \approx 2[(\gamma_2 + 1)/2\gamma_2]^{-(\gamma_2 + 1)/2(\gamma_2 - 1)} \quad (15)$$

If the one-γ model were adopted, the duration of the thrust plateau would be given by

$$t_{plateau}|_{\gamma_1 = \gamma_2 = \gamma} = 2\left(\frac{M_{CJ}^2 + 1}{\gamma M_{CJ}^2 + 1}\frac{\gamma + 1}{2}\right)^{-(\gamma + 1)/2(\gamma - 1)} t_{CJ} \quad (16a)$$

This result was derived in Ref. 8. Further, when $M_{CJ}^2 \gg 1$, this would become

$$t_{plateau}|_{\gamma_1 = \gamma_2 = \gamma, M_{CJ}^2 \gg 1} \approx 2[(\gamma + 1)/2\gamma]^{-(\gamma + 1)/2(\gamma - 1)} t_{CJ} \quad (16b)$$

This result was derived in Ref. 4.

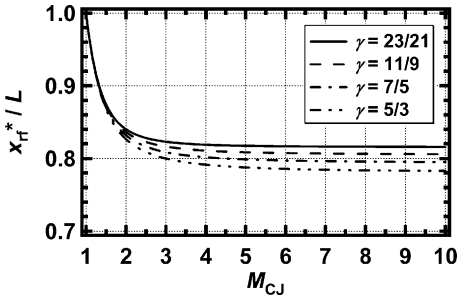

Fig. 4 Dependence of x_{rf}^*/L on M_{CJ} and γ, where $\gamma_1 = \gamma_2 = \gamma$ was assumed.

Decay in the Thrust History

Next, we formulate the decay portion of the pressure history at the thrust wall. This formulation is the most significant in this work. First, we think about flowfield in the tube just before the time $t_{plateau}$. If $x_{rf}^* \approx L$, the exhausting rarefaction wave should be a self-similar rarefaction wave propagating from the open end toward the closed end through the uniform gas characterized by $\gamma_3 (= \gamma_2)$, p_3, a_3, and $u_3 (= 0)$. We call this self-similar rarefaction wave the approximate self-similar rarefaction wave hereafter. And if $L - x_{rf}^* \ll L$, the flowfield in the tube just before the time $t_{plateau}$ can be close to that of the approximate self-similar rarefaction wave. Figure 4 shows the dependence of x_{rf}^*/L on M_{CJ} and γ, where we assumed that $\gamma_1 = \gamma_2 = \gamma$. As shown in Fig. 4, the dependence of x_{rf}^*/L on γ is weak, and the condition $L - x_{rf}^* \ll L$ is almost satisfied. In the limit that $M_{CJ}^2 \to 1$, x_{rf}^*/L is given by

$$\left.\frac{x_{rf}^*}{L}\right|_{M_{CJ}^2 \to 1} \approx \frac{1}{2}\frac{\gamma_1 + \gamma_2}{\gamma_1}\left(\frac{\gamma_1 + \gamma_2}{\gamma_1 + 1}\frac{\gamma_2 + 1}{2\gamma_2}\right)^{-(\gamma_2 + 1)/2(\gamma_2 - 1)} \quad (17a)$$

In this limit, we can also consider that $\gamma_1 \approx \gamma_2$. Therefore, we can write as follows:

$$\left(x_{rf}^*/L\right)\big|_{M_{CJ}^2 \to 1} \approx 1 \quad (17b)$$

On the other hand, x_{rf}^*/L in the limit that $M_{CJ}^2 \gg 1$ is given by

$$\left(x_{rf}^*/L\right)\big|_{M_{CJ}^2 \gg 1} \approx \tfrac{1}{2}[(\gamma_2 + 1)/2\gamma_2]^{-(\gamma_2 + 1)/2(\gamma_2 - 1)} \quad (18)$$

In the range that $1 < \gamma_2 \le \frac{5}{3}$, this is a monotonically decreasing function of γ_2 and ranges between $25/32 \approx 0.781$ and 0.825. Based on the preceding estimation, we consider the interference between the exhausting rarefaction wave and its reflection from the closed end as that between the approximate self-similar rarefaction wave and its reflection from the closed end in the following analysis. The validity of this approximation will be further examined later in the section in which we will describe comparison between the analytical and numerical results.

Here, we briefly summarize the gas dynamics of the approximate self-similar rarefaction wave, the front boundary of which reaches the closed end at the time $t_{plateau}$. The following results are obtained by using the results in Ref. 12. The pressure, sound speed, and flow velocity in the approximate self-similar rarefaction wave are, respectively, given by

$$p = \left(\frac{2}{\gamma_2 + 1} + \frac{\gamma_2 - 1}{\gamma_2 + 1}\frac{L - x}{a_3 t - a_3 t_{plateau} + L}\right)^{2\gamma_2/(\gamma_2 - 1)} p_3 \quad (19a)$$

$$a = \frac{2}{\gamma_2 + 1} a_3 + \frac{\gamma_2 - 1}{\gamma_2 + 1}\frac{L - x}{t - t_{plateau} + L/a_3} \quad (19b)$$

$$u = a - \frac{L - x}{t - t_{plateau} + L/a_3} \le a \quad (19c)$$

Table 1 Function describing the decay portion of the pressure history at the thrust wall

n	γ_2	f_n
1	$\frac{5}{3}=1.667$	$f_1\left(\frac{p_3}{p_w}\right) = \frac{1}{2}\left(\frac{p_3}{p_w}\right)^{\frac{1}{5}} + \frac{1}{2}\left(\frac{p_3}{p_w}\right)^{\frac{3}{5}}$
2	$\frac{7}{5}=1.4$	$f_2\left(\frac{p_3}{p_w}\right) = \frac{3}{2^3}\left(\frac{p_3}{p_w}\right)^{\frac{1}{7}} + \frac{1}{2^2}\left(\frac{p_3}{p_w}\right)^{\frac{3}{7}} + \frac{3}{2^3}\left(\frac{p_3}{p_w}\right)^{\frac{5}{7}}$
3	$\frac{9}{7}=1.286$	$f_3\left(\frac{p_3}{p_w}\right) = \frac{5}{2^4}\left(\frac{p_3}{p_w}\right)^{\frac{1}{9}} + \frac{3}{2^4}\left(\frac{p_3}{p_w}\right)^{\frac{3}{9}} + \frac{3}{2^4}\left(\frac{p_3}{p_w}\right)^{\frac{5}{9}} + \frac{5}{2^4}\left(\frac{p_3}{p_w}\right)^{\frac{7}{9}}$
4	$\frac{11}{9}=1.222$	$f_4\left(\frac{p_3}{p_w}\right) = \frac{35}{2^7}\left(\frac{p_3}{p_w}\right)^{\frac{1}{11}} + \frac{5}{2^5}\left(\frac{p_3}{p_w}\right)^{\frac{3}{11}} + \frac{9}{2^6}\left(\frac{p_3}{p_w}\right)^{\frac{5}{11}} + \frac{5}{2^5}\left(\frac{p_3}{p_w}\right)^{\frac{7}{11}} + \frac{35}{2^7}\left(\frac{p_3}{p_w}\right)^{\frac{9}{11}}$
6	$\frac{15}{13}=1.154$	$f_6\left(\frac{p_3}{p_w}\right) = \frac{231}{2^{10}}\left(\frac{p_3}{p_w}\right)^{\frac{1}{15}} + \frac{63}{2^9}\left(\frac{p_3}{p_w}\right)^{\frac{3}{15}} + \frac{105}{2^{10}}\left(\frac{p_3}{p_w}\right)^{\frac{5}{15}} + \frac{25}{2^8}\left(\frac{p_3}{p_w}\right)^{\frac{7}{15}} + \frac{105}{2^{10}}\left(\frac{p_3}{p_w}\right)^{\frac{9}{15}} + \frac{63}{2^9}\left(\frac{p_3}{p_w}\right)^{\frac{11}{15}} + \frac{231}{2^{10}}\left(\frac{p_3}{p_w}\right)^{\frac{13}{15}}$
10	$\frac{23}{21}=1.095$	$f_{10}\left(\frac{p_3}{p_w}\right) = \frac{46,189}{2^{18}}\left(\frac{p_3}{p_w}\right)^{\frac{1}{23}} + \frac{12,155}{2^{17}}\left(\frac{p_3}{p_w}\right)^{\frac{3}{23}} + \frac{19,305}{2^{18}}\left(\frac{p_3}{p_w}\right)^{\frac{5}{23}} + \frac{2145}{2^{15}}\left(\frac{p_3}{p_w}\right)^{\frac{7}{23}} + \frac{8085}{2^{17}}\left(\frac{p_3}{p_w}\right)^{\frac{9}{23}} + \frac{3969}{2^{16}}\left(\frac{p_3}{p_w}\right)^{\frac{11}{23}} + \frac{8085}{2^{17}}\left(\frac{p_3}{p_w}\right)^{\frac{13}{23}} + \frac{2145}{2^{15}}\left(\frac{p_3}{p_w}\right)^{\frac{15}{23}} + \frac{19,305}{2^{18}}\left(\frac{p_3}{p_w}\right)^{\frac{17}{23}} + \frac{12,155}{2^{17}}\left(\frac{p_3}{p_w}\right)^{\frac{19}{23}} + \frac{46,189}{2^{18}}\left(\frac{p_3}{p_w}\right)^{\frac{21}{23}}$

These quantities at the open end ($x = L$) are, respectively, kept to be

$$p|_{x=L} = [2/(\gamma_2+1)]^{2\gamma_2/(\gamma_2-1)} p_3 \tag{20a}$$

$$a|_{x=L} = [2/(\gamma_2+1)] a_3 \tag{20b}$$

$$u|_{x=L} = a|_{x=L} \tag{20c}$$

Next, we describe the formulation of the decay portion of the pressure history at the thrust wall, that is, the pressure history at the thrust wall in the time region $t_{\text{plateau}} < t$. Let us recall the approximation that the interference between the exhausting rarefaction wave and its reflection from the closed end is replaced with that between the self-similar rarefaction wave propagating from the open end toward the closed end through the uniform gas characterized by $\gamma_3(=\gamma_2)$, p_3, a_3, and $u_3(=0)$ and its reflection from the closed end. In fact, we can find this approximate situation in problem 1 in Ref. 13. According to Ref. 13, when the front boundary of the approximate self-similar rarefaction wave reaches the closed end of the tube with length L at the time t_{plateau}, the state of the gas at the closed end after the time t_{plateau} is analytically given by

$$t - \left(t_{\text{plateau}} - \frac{L}{a_3}\right) = \frac{L}{2^n n!}\left(\frac{1}{a_w}\frac{\partial}{\partial a_w}\right)^n \left[\frac{1}{a_w}\left(a_w^2 - a_3^2\right)^n\right] \tag{21}$$

That is, strictly speaking, analytical solutions exist for only discrete values of γ_2. By using the preceding solution and an isentropic relation

$$a_3^2 \big/ a_w^2 = (p_w/p_3)^{-2/(2n+3)} \tag{22}$$

the decay portion of the pressure history at the thrust wall for a positive integer n can be formulated as follows:

$$a_3(t - t_{\text{plateau}})/L + 1 = f_n(p_3/p_w) \tag{23}$$

where the function f_n is as shown in Table 1. Figure 5 shows decay histories of the pressure at the thrust wall for several values of γ_2. As shown in Fig. 5, the dependency of the thrust-decay history on γ_2 is not strong so much.

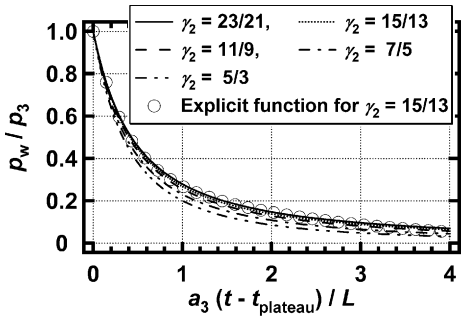

Fig. 5 Decay history of the pressure at the thrust wall.

Because it is inconvenient that the thrust-decay histories are given for only positive integers n, namely, for only discrete values of γ_2, we use approximate thrust-decay histories for arbitrary values of γ_2. The approximate thrust-decay history for an arbitrary value of γ_2 is given by interpolating or extrapolating two f_ns for appropriate values of n shown in Table 1, which are denoted by n_a and n_b, namely, given by

$$a_3(t - t_{\text{plateau}})/L + 1 = f_{n'}(p_3/p_w) \tag{24a}$$

where

$$n' = (3 - \gamma_2)/2(\gamma_2 - 1) \tag{24b}$$

$$f_{n'}(p_3/p_w) = (1 - X) f_{n_a}(p_3/p_w) + X f_{n_b}(p_3/p_w) \tag{24c}$$

$$X = (\gamma_2 - \gamma_a)/(\gamma_b - \gamma_a) \tag{24d}$$

$$\gamma_a = (2n_a + 3)/(2n_a + 1) \tag{24e}$$

$$\gamma_b = (2n_b + 3)/(2n_b + 1) \tag{24f}$$

Furthermore, it is sometimes convenient that the thrust-decay histories are given by explicit functions of time. For that purpose, we determine the following explicit function of time, which satisfies

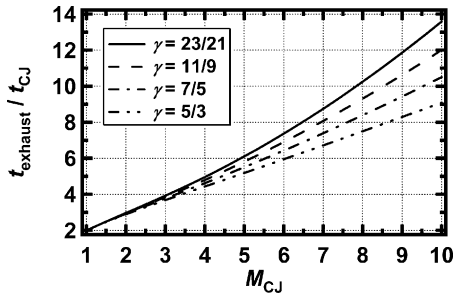

Fig. 6 Dependence of $t_{exhaust}/t_{CJ}$ on M_{CJ} and γ, where $\gamma_1 = \gamma_2 = \gamma$ was assumed.

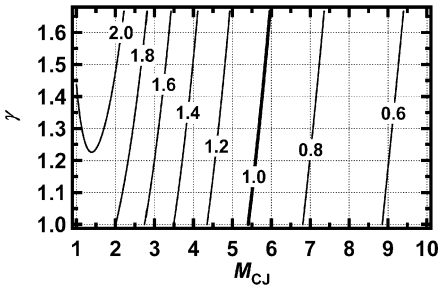

Fig. 7 Contour plot of $t'_{valid}/t_{exhaust}$ in M_{CJ}-γ plane, where $\gamma_1 = \gamma_2 = \gamma$ was assumed.

the condition that $p_w = p_3$ when $t = t_{plateau}$, by fitting the implicit function of time:

$$p_w/p_3 = k_A \exp[-k_B(a_3/L)(t - t_{plateau})] + (1 - k_A)\exp[-k_C(a_3/L)(t - t_{plateau})] \quad (25)$$

where k_A, k_B, and k_C are numerical constants determined by χ-square minimization. Because the dependency of the thrust-decay history on γ_2 is not strong as already mentioned, we actually determined k_A, k_B, and k_C by the fitting of the implicit function for $n = 6$ only, namely, for $\gamma_2 = 15/13 \approx 1.154$ only. The results of the fitting are $k_A = 0.6066$, $k_B = 2.991$ and $k_C = 0.5014$. This explicit function was also shown in Fig. 5.

Denoting the time at which $p_w = p_1$ by $t_{exhaust}$, $t_{exhaust}$ is obtained by substituting $t_{exhaust}$ and p_1 for t and p_w in Eq. (24a), respectively, and given by

$$t_{exhaust} = \{\delta_{A2}[f_{n'}(\delta_{A1}) - 1] + \delta_B\}t_{CJ} \quad (26)$$

Figure 6 shows the dependence of $t_{exhaust}/t_{CJ}$ on M_{CJ} and γ, where we assumed that $\gamma_1 = \gamma_2 = \gamma$.

Finally, we roughly estimate the condition for that the obtained results are valid. Denoting the boundary of the interference region between the exhausting rarefaction wave and its reflection from the closed end by x_{ir}, x_{ir} is the leading characteristic propagating from the closed end toward the open end in the exhausting rarefaction wave. This characteristic starts to propagate at the time $t_{plateau}$. Let us recall again the approximation that the interference between the exhausting rarefaction wave and its reflection from the closed end is replaced with that between the approximate self-similar rarefaction wave and its reflection from the closed end. Because of this approximation, the sound speed and the flow velocity in the exhausting rarefaction wave were given by Eqs. (19b) and (19c), respectively. Because x_{ir} is the leading characteristic propagating from the closed end toward the open end in the exhausting rarefaction wave, x_{ir} is governed by the following equation:

$$\frac{dx_{ir}}{dt} = u + a = \frac{4}{\gamma_2 + 1}a_3 - \frac{3 - \gamma_2}{\gamma_2 + 1}\frac{L - x_{ir}}{t - t_{plateau} + L/a_3} \quad (27)$$

Solving this differential equation with the condition that $x_{ir} = 0$ when $t = t_{plateau}$, the following solution is obtained:

$$x_{ir} = L - \frac{\gamma_2 + 1}{\gamma_2 - 1}a_3\left(t - t_{plateau} + \frac{L}{a_3}\right) \times \left\{\left[\left(t - t_{plateau} + \frac{L}{a_3}\right)\frac{a_3}{L}\right]^{-2(\gamma_2 - 1)/(\gamma_2 + 1)} - \frac{2}{\gamma_2 + 1}\right\} \quad (28)$$

Denoting the time at which $x_{ir} = L$ by $t^{\#}$, $t^{\#}$ is given by

$$t^{\#} = \left(\delta_B + \delta_{A2}\left\{[2/(\gamma_2 + 1)]^{-(\gamma_2 + 1)/2(\gamma_2 - 1)} - 1\right\}\right)t_{CJ} \quad (29)$$

As far as no strong shock wave enters the tube, the obtained thrust-decay history is valid until the time t_{valid} at which the leading characteristic, which starts to propagate from the open end toward the closed end at the time $t^{\#}$, reaches the closed end.

Let us roughly estimate the time t_{valid}. Because of the isentropic process, sound speed relates to pressure as

$$a = a_3(p/p_3)^{(\gamma_2 - 1)/2\gamma_2} \quad (30)$$

Regarding the power in the preceding relation, $0 < (\gamma_2 - 1)/(2\gamma_2) \leq \frac{1}{5}$ in the case of $1 < \gamma_2 \leq \frac{5}{3}$. Accordingly, the variation of the sound speed in the tube is so small. Based on the smallness of the variation of the sound speed in the tube, we estimate the time t'_{valid} instead of t_{valid}, where t'_{valid} is defined by

$$L = \int_{t^{\#}}^{t'_{valid}} a_w \, dt \quad (31)$$

Because the gas in the tube is flowing in the direction from the closed end to the open end, the time t'_{valid}, in the definition of which the flow velocity was neglected, can be much earlier than the time t_{valid}. In Eq. (31), the sound speed at the thrust wall is given by

$$a_w = a_3(p_w/p_3)^{(\gamma_2 - 1)/2\gamma_2} \quad (32)$$

As mentioned earlier, the power in Eq. (32), namely, $(\gamma_2 - 1)/(2\gamma_2)$, is small. Therefore, the dependency of a_w on p_w/p_3 is weak. Furthermore, as shown in Fig. 5, the dependency of p_w/p_3 on γ_2 is not so strong. Based on these, we use the approximate explicit function (25) and the numerical constants determined by fitting the implicit function for $n = 6$ ($\gamma_2 = 15/13 \approx 1.154$) in calculating t'_{valid}, namely, we use

$$a_w = a_3\{k_A \exp[-k_B(a_3/L)(t - t_{plateau})] + (1 - k_A)\exp[-k_C(a_3/L)(t - t_{plateau})]\}^{(\gamma_2 - 1)/2\gamma_2} \quad (33)$$

and $k_A = 0.6066$, $k_B = 2.991$, and $k_C = 0.5014$ in calculating t'_{valid}. The condition $t'_{valid}/t_{exhaust} \geq 1$ is a sufficient condition for that the obtained thrust-decay history is valid. The dependence of $t'_{valid}/t_{exhaust}$ on M_{CJ} and γ, where we assumed that $\gamma_1 = \gamma_2 = \gamma$, is shown in Fig. 7. The condition $t'_{valid}/t_{exhaust} \geq 1$ is a sufficient condition for the validity of the obtained thrust-decay history. As shown in Fig. 7, a sufficient condition for the validity of the obtained thrust-decay history is approximately given by $M_{CJ} < 5.5$. The validity of the obtained thrust-decay history in the case of $M_{CJ} > 5.5$ should be examined by comparing the obtained analytical formulas with results of experiments or numerical simulations.

Performance Parameters

In this subsection, we formulate the impulse per unit cross section per one cycle and the specific impulse of a simplified PDE by integrating the obtained pressure history at the thrust wall with respect to time. From Eq. (2), we can write the impulse per unit cross section per one cycle of a simplified PDE as follows:

$$I_{cyc} = (p_3 - p_1)\,t_{plateau} + \int_{t_{plateau}}^{t_{exhaust}} (p_w - p_1)dt + (p_1 - p_{out})\tau \quad (34)$$

Table 2 Function describing I_{cyc}

n	γ_2	F_n
1	$\frac{5}{3}=1.667$	$F_1(\delta_{A1},\delta_{A2})=\frac{\delta_{A2}}{\delta_{A1}-1}\left(\frac{7}{2^3}\delta_{A1}-\frac{5}{2^3}\delta_{A1}^{\frac{1}{5}}-\frac{5}{2^2}\delta_{A1}^{\frac{3}{5}}+1\right)$
2	$\frac{7}{5}=1.4$	$F_2(\delta_{A1},\delta_{A2})=\frac{\delta_{A2}}{\delta_{A1}-1}\left(\frac{19}{2^4}\delta_{A1}-\frac{7}{2^4}\delta_{A1}^{\frac{1}{7}}-\frac{7}{2^4}\delta_{A1}^{\frac{3}{7}}-\frac{21}{2^4}\delta_{A1}^{\frac{5}{7}}+1\right)$
3	$\frac{9}{7}=1.286$	$F_3(\delta_{A1},\delta_{A2})=\frac{\delta_{A2}}{\delta_{A1}-1}\left(\frac{187}{2^7}\delta_{A1}-\frac{45}{2^7}\delta_{A1}^{\frac{1}{9}}-\frac{9}{2^5}\delta_{A1}^{\frac{3}{9}}-\frac{27}{2^6}\delta_{A1}^{\frac{5}{9}}-\frac{45}{2^5}\delta_{A1}^{\frac{7}{9}}+1\right)$
4	$\frac{11}{9}=1.222$	$F_4(\delta_{A1},\delta_{A2})=\frac{\delta_{A2}}{\delta_{A1}-1}\left(\frac{437}{2^8}\delta_{A1}-\frac{77}{2^8}\delta_{A1}^{\frac{1}{11}}-\frac{55}{2^8}\delta_{A1}^{\frac{3}{11}}-\frac{33}{2^7}\delta_{A1}^{\frac{5}{11}}-\frac{55}{2^7}\delta_{A1}^{\frac{7}{11}}-\frac{385}{2^8}\delta_{A1}^{\frac{9}{11}}+1\right)$
6	$\frac{15}{13}=1.154$	$F_6(\delta_{A1},\delta_{A2})=\frac{\delta_{A2}}{\delta_{A1}-1}\left(\begin{array}{c}\frac{4387}{2^{11}}\delta_{A1}-\frac{495}{2^{11}}\delta_{A1}^{\frac{1}{15}}-\frac{315}{2^{11}}\delta_{A1}^{\frac{3}{15}}-\frac{315}{2^{11}}\delta_{A1}^{\frac{5}{15}}-\frac{375}{2^{11}}\delta_{A1}^{\frac{7}{15}}\\ -\frac{525}{2^{11}}\delta_{A1}^{\frac{9}{15}}-\frac{945}{2^{11}}\delta_{A1}^{\frac{11}{15}}-\frac{3465}{2^{11}}\delta_{A1}^{\frac{13}{15}}+1\end{array}\right)$
10	$\frac{23}{21}=1.095$	$F_{10}(\delta_{A1},\delta_{A2})=\frac{\delta_{A2}}{\delta_{A1}-1}\left(\begin{array}{c}\frac{1,503,829}{2^{19}}\delta_{A1}-\frac{96,577}{2^{19}}\delta_{A1}^{\frac{1}{23}}-\frac{55,913}{2^{19}}\delta_{A1}^{\frac{3}{23}}-\frac{49,335}{2^{19}}\delta_{A1}^{\frac{5}{23}}-\frac{49,335}{2^{19}}\delta_{A1}^{\frac{7}{23}}-\frac{26,565}{2^{18}}\delta_{A1}^{\frac{9}{23}}-\frac{30,429}{2^{18}}\delta_{A1}^{\frac{11}{23}}\\ -\frac{37,191}{2^{18}}\delta_{A1}^{\frac{13}{23}}-\frac{49,335}{2^{18}}\delta_{A1}^{\frac{15}{23}}-\frac{148,005}{2^{19}}\delta_{A1}^{\frac{17}{23}}-\frac{279,565}{2^{19}}\delta_{A1}^{\frac{19}{23}}-\frac{1,062,347}{2^{19}}\delta_{A1}^{\frac{21}{23}}+1\end{array}\right)$

Because the thrust-decay history is given by an implicit function of time, we rewrite the second term in the right-hand side of the preceding equation as follows:

$$I_{cyc}=\delta_B(p_3-p_1)t_{CJ}+\int_{p_1}^{p_3}(t-t_{plateau})\,dp_w+(p_1-p_{out})\tau \quad (35)$$

where Eq. (13) was used for $t_{plateau}$. By calculating the second term in the right-hand side of the preceding equation, I_{cyc} for a positive integer n is formulated as follows;

$$I_{cyc}=[\delta_B+F_n(\delta_{A1},\delta_{A2})](p_3-p_1)t_{CJ}+(p_1-p_{out})\tau \quad (36)$$

where the function F_n is as shown in Table 2. As is the case with the thrust-decay history, the approximate impulse for an arbitrary value of γ_2 is given by interpolating or extrapolating two $F_n s$ for appropriate values of n shown in Table 2, which are denoted by n_a and n_b, namely, given by

$$I_{cyc}=[\delta_B+F_{n'}(\delta_{A1},\delta_{A2})](p_3-p_1)t_{CJ}+(p_1-p_{out})\tau \quad (37a)$$

where

$$F_{n'}(\delta_{A1},\delta_{A2})=(1-X)F_{n_a}(\delta_{A1},\delta_{A2})+XF_{n_b}(\delta_{A1},\delta_{A2}) \quad (37b)$$

and n', X, γ_a, and γ_b are given by Eqs. (24b), (24d), (24e), and (24f), respectively.

Although the impulse per unit cross section per one cycle of a PDE is formulated as Eq. (37a), only the contribution by positive overpressure often has an engineering significance. From this viewpoint, we denote the impulse per unit cross section per one cycle contributed by positive overpressure by $I_{cyc(+)}$, which is given by

$$I_{cyc(+)}=[\delta_B+F_{n'}(\delta_{A1},\delta_{A2})](p_3-p_1)t_{CJ} \quad (38)$$

Figure 8 shows the dependence of $I_{cyc(+)}/[(p_3-p_1)t_{CJ}]$ on M_{CJ} and γ, where we assumed that $\gamma_1=\gamma_2=\gamma$.

Finally, the mixture-based and fuel-based specific impulses of a simplified PDE are, respectively, formulated as follows:

$$I_{sp}=\frac{I_{cyc}}{\rho_1 Lg}=I_{sp(+)}+\frac{(p_1-p_{out})\tau}{\rho_1 Lg} \quad (39a)$$

$$I_{spf}=\frac{I_{cyc}}{\phi_f\rho_1 Lg}=I_{spf(+)}+\frac{(p_1-p_{out})\tau}{\phi_f\rho_1 Lg} \quad (39b)$$

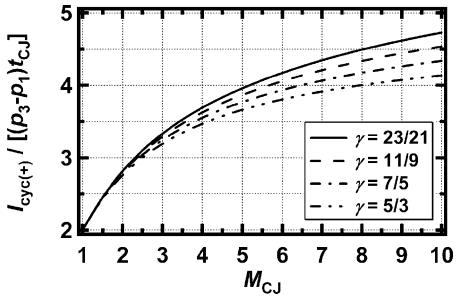

Fig. 8 Dependence of nondimensional $I_{cyc(+)}$ on M_{CJ} and γ, where $\gamma_1=\gamma_2=\gamma$ was assumed.

where

$$I_{sp(+)}=\frac{I_{cyc(+)}}{\rho_1 Lg} \quad (40a)$$

$$I_{spf(+)}=\frac{I_{cyc(+)}}{\phi_f\rho_1 Lg} \quad (40b)$$

Summary of the Formulation

The pressure history at the thrust wall p_w and the performance parameters $t_{exhaust}$, I_{cyc}, I_{sp}, and I_{spf} can be calculated from the parameters γ_1, γ_2, M_{CJ}, D_{CJ}, L, p_1, p_{out}, τ, ρ_1, and ϕ_f by the following procedure. First, we calculate t_{CJ}, δ_{A1}, δ_{A2}, δ_B, and n' by using Eqs. (4), (7a), (7b), (14), and (24b), respectively. Next, we determine appropriate values of n_a and n_b from the value of n' and by using Table 1 or 2, and calculate γ_a, γ_b, and X by using Eqs. (24e), (24f), and (24d), respectively. After that, we calculate p_3, a_3, and $t_{plateau}$ by using Eqs. (6a), (6b), and (13), respectively. The pressure history at the thrust wall is given by

$$p_w(t;\,0<t\le t_{plateau})=p_3 \quad (41a)$$

$$t(p_w;\,p_1\le p_w<p_3)=(L/a_3)[f_{n'}(p_3/p_w)-1]+t_{plateau} \quad (41b)$$

with Eq. (24c). Equation (41a) shows the plateau in the pressure history at the thrust wall, and Eq. (41b) shows the following decay, which is given by time implicitly. On the performance parameters, we calculate $t_{exhaust}$, I_{cyc}, I_{sp}, and I_{spf} by using Eqs. (26), (37a), (39a), and (39b), respectively, with Eqs. (24c) and (37b).

Table 3 Parameters for theoretical formulas

Gas mixture	γ_1	γ_2	M_{CJ}	D_{CJ}[a]
$H_2 + air$ (stoichiometric)	1.394	1.167	4.852	1979
$2H_2 + O_2$	1.396	1.129	5.276	2841
$C_2H_4 + 3O_2 + N_2$	1.341	1.139	6.844	2269
$C_2H_4 + 3O_2$	1.329	1.140	7.267	2376
$C_2H_2 + 2.5O_2$	1.324	1.153	7.344	2425

[a]In meters/second.

On the parameters needed for calculations of the pressure history at the thrust wall and the performance parameters, p_{out}, L, τ, ϕ_f, p_1, and ρ_1 are generally given as the operation condition of a PDE. And also the initial temperature T_1 is known from p_1 and ρ_1 through the equation of state. Once the species and thermodynamic state of the undisturbed detonable gas are determined, we can determine γ_1, γ_2, M_{CJ}, and D_{CJ} by calculations based on the conservation laws of gas dynamics and the chemical equilibrium of the unburned and burned gases. Table 3 shows some sets of these parameters, which will be used later in comparison between the obtained formulas and numerical and/or experimental results. These parameters were obtained for the condition that $p_1 = 0.101325$ MPa (1 atm) and $T_1 = 300$ K by using the chemical-equilibrium code STANJAN,[14] where we substituted $O_2 + 3.76N_2$ for the air.

Here, we have to explain how to determine the parameters γ_1 and γ_2 in detail. The parameter γ_1 is determined by using the relation $a_1^2 = \gamma_1 p_1/\rho_1$, where a_1 is the frozen sound speed of the undisturbed detonable gas. On the other hand, the parameter γ_2 is determined by using the relation $a_2^2 = \gamma_2 p_2/\rho_2$, where a_2 is the equilibrium sound speed of the burned gas at the rear surface of the CJ detonation wave. The use of the relation $a^2 = \gamma p/\rho$ corresponds to adopting the approximation that the change of the thermodynamic variables of the gas is regarded as the polytropic change except for the inside of the detonation wave. That is, we adopt the approximation that the relations $p/\rho^\gamma = p_1/\rho_1^{\gamma_1}$ and $p/\rho^\gamma = p_2/\rho_2^{\gamma_2} = p_3/\rho_3^{\gamma_2}$ hold for the unburned and burned gases, respectively. To be exact, γ is more appropriate to be called the polytropic index than the specific-heat ratio in this case. Generally, the chemical composition of the unburned gas is frozen. Therefore, for the unburned gas the polytropic index is practically the same as the specific-heat ratio. However, the temperature of the gas burned as a detonation wave is, in general, so high that its chemical equilibrium is attained rapidly. Furthermore, the relation $p/\rho^\gamma = p_2/\rho_2^{\gamma_2} = p_3/\rho_3^{\gamma_2}$ played important roles in the analysis of the gas dynamics of the burned gas. These are the reasons why we determine the parameter γ_2 by using the relation $a_2^2 = \gamma_2 p_2/\rho_2$, where a_2 is the equilibrium sound speed of the burned gas at the rear surface of the CJ detonation wave. As shown in Table 3, the typical value of n (γ_2) is $n = 6$ ($\gamma_2 = 15/13 \approx 1.154$).

Comparison with Numerical Simulations, Experiments, and Semi-Empirical Formulas

Comparison with Numerical Simulations

For validation of the obtained analytical formulas, we compared them with results of numerical simulations. Figure 9 shows the geometrical conditions of the numerical simulations. The computational domain was axisymmetric. We carried out numerical simulations in two cases: case 1 is that $L = 100$ mm and $r = 5$ mm, and case 2 is that $L = 100$ mm and $r = 2.5$ mm. In the time region $0 \le t \le t_{CJ} = L/D_{CJ}$, flowfield in the tube only was calculated one dimensionally along the axis of the tube. Only after the time t_{CJ}, flowfield in the whole computational domain shown in Fig. 9 was calculated axisymmetrically. The initial gas pressure and temperature were, respectively, 0.101325 MPa (1 atm) and 300 K in the whole computational domain. In the hydrodynamic code,[15] we adopted an elementary-reaction model[16] for calculating the heat release and the chemical composition right through, where nitrogen was treated to be inert. For initiation of the detonation wave, we artificially set up a thin high-pressure region, which was 3 MPa in pressure, 3000 K in temperature, and 0.4 mm in thickness, on the thrust wall. All numerical results shown next are the values on the central axis of the tube.

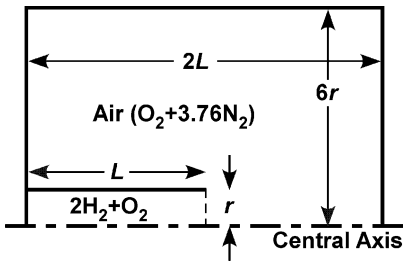

Fig. 9 Geometrical conditions of numerical simulations.

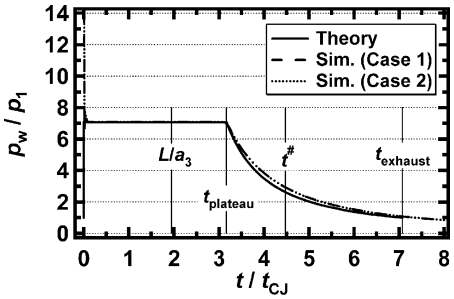

Fig. 10 Comparison between the analytical and numerical results on the pressure history at the thrust wall.

Figure 10 shows comparison between the analytical and numerical results on the pressure history at the thrust wall. Some characteristic times in the theoretical analysis were also shown in Fig. 10. The numerical results in the two cases were almost completely in agreement each other, showing that the obtained numerical results were independent of the aspect ratio of the tube L/r. It is not surprising that the theoretical result had no initial peak although the numerical results had it because the initiation of the detonation wave was not treated in the theoretical analysis. Although the theoretically predicted pressure was just a little lower than the numerical results in the decay portion, the theoretical result and the numerical results were in very good agreement as a whole. In other words, the disagreement in the decay portion represents the limit of the accuracy of the analytical formulas. On the mixture-based specific impulse, the analytical result was $I_{sp} = 186.3$ s. Correspondingly, the numerical result was $I_{sp} = 195.0$ s, which included the initial peak and was higher than the analytical result by 4.7%, or $I_{sp} = 192.6$ s, which did not include the initial peak, where

$$\int_0^{t_{CJ}} \Delta p \, dt$$

was replaced by

$$2\int_{t_{CJ}/2}^{t_{CJ}} \Delta p \, dt$$

and was higher than the analytical result by 3.4%.

Figure 11 shows the histories of pressure and Mach number at the open end of the tube. Some characteristic times in the theoretical analysis were also shown in Fig. 11. In the theoretical analysis, we adopted the approximation that the interference between the exhausting rarefaction wave and its reflection from the closed end is replaced by that between the approximate self-similar rarefaction wave and its reflection from the closed end. If this approximation is appropriate, the pressure at the open end ought to come close to a definite value given by Eq. (20a), which was $2.37p_1$ in this case, when time gets closer to $t_{plateau}$, and after the time $t_{plateau}$, the pressure at the open end ought to be kept at that definite value until the time $t^\#$. And the Mach number at the open end ought to come close to unity when time gets closer to $t_{plateau}$, and after the time $t_{plateau}$, the Mach number at the open end ought to be kept at unity until the time

Table 4 Comparison between the theoretical and experimental results on specific impulse

Ref.	Gas mixture	Initiation	Frequency	Experiment[a]	Theory[a]
5	$H_2 + \text{air}$ (stoichiometric)	Spark plugs and Shchelkin spiral	16 Hz	$I_{spf} = 3800 \sim 4450$	$I_{spf} = 4215$
6	$2H_2 + O_2$	Spark plug only	Single pulse	$I_{sp} = 191$	$I_{sp} = 186.3$
6, 7	$C_2H_4 + 3O_2 + N_2$	Spark plug only	Single pulse	$I_{sp} = 159$	$I_{sp} = 160.8$
6, 7	$C_2H_4 + 3O_2$	Spark plug only	Single pulse	$I_{sp} = 171$	$I_{sp} = 171.2$
6	$C_2H_2 + 2.5O_2$	Spark plug only	Single pulse	$I_{sp} = 202$	$I_{sp} = 172.7$
3	$C_2H_2 + 2.5O_2$	Initiating tube	Single pulse	$I_{sp} = 193 \sim 203$	$I_{sp} = 172.7$

[a] I_{spf}, I_{sp} in seconds.

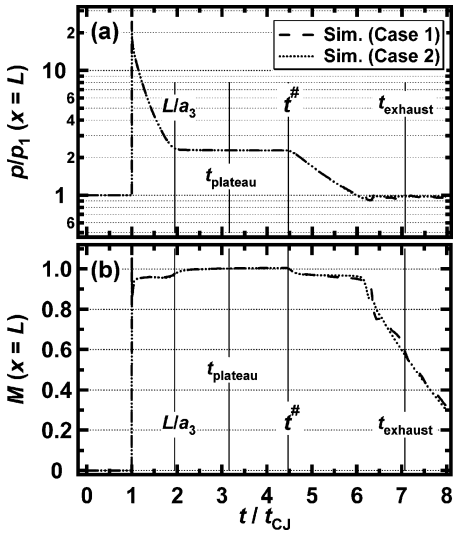

Fig. 11 Numerically calculated histories of a) pressure and b) Mach number at the open end of the tube.

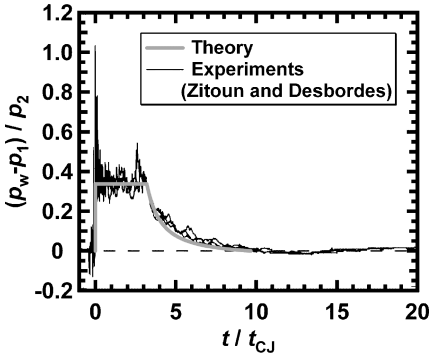

Fig. 12 Comparison between the theoretical and experimental results on the pressure history at the thrust wall.

$t^{\#}$. As shown in Fig. 11, the numerical results showed that almost in the time region $L/a_3 < t < t^{\#}$, the pressure at the open end was kept at a definite value, which was $2.29\,p_1$ and agreed with the theoretical prediction with 3.4% accuracy, and the Mach number at the open end was kept at unity. This shows the validity of the approximation that the interference between the exhausting rarefaction wave and its reflection from the closed end was replaced by that between the approximate self-similar rarefaction wave and its reflection from the closed end.

Further, the numerical results shown in Fig. 11 show that the Mach number at the open end is kept at almost unity until when the pressure at the open end comes down to the ambient pressure even after the time $t^{\#}$. This shows that a small disturbance, which starts to propagate from the open end toward the closed end at the time $t^{\#}$, can propagate toward the closed end only with much lower speed than the sound speed. Accordingly, the earlier-discussed sufficient condition for the validity of the obtained results, which was $t'_{\text{valid}}/t_{\text{exhaust}} \geq 1$ in Fig. 7, is too sufficient, and the parameter region, in which the obtained results are valid, is more extensive than that shown by $t'_{\text{valid}}/t_{\text{exhaust}} \geq 1$ in Fig. 7.

Comparison with Experiments and Semi-Empirical Formulas

Further, we compared the obtained theoretical formulas with published experimental results. Figure 12 shows comparison between the theoretical and experimental results on the pressure history at the thrust wall. The experimental results shown in Fig. 12 were obtained by Zitoun and Desbordes.[4] In their experiments, the detonable gas mixture was C_2H_4+$3O_2$, and it was initially at ambient conditions of pressure and temperature. As shown in Fig. 12, the theoretical formulas, Eqs. (41a) and (41b), were in good agreement with the experimental results as a whole. As is the case with the comparison between the analytical and numerical results, the theoretically predicted pressure at the thrust wall was just a little lower than the experimental results in the decay portion.

In Table 4, we summarize available experimental data and the corresponding theoretical predictions on specific impulse. In all experiments shown in Table 4, the detonable gas mixtures were initially at ambient conditions of pressure and temperature. The theoretical predictions were in agreement with the experimental data within a few percent except for the case of C_2H_2+$2.5O_2$. In the case of C_2H_2+$2.5O_2$, the theoretical prediction was lower than the experimental data by about 15%. Although the reason of this disagreement is not yet clarified, one possibility is the impurity of the detonable gas mixture, C_2H_2+$2.5O_2$, because obtaining of high-purity acetylene is generally not so easy because of solvent.

Finally, we compare this work with the semi-empirical models recently proposed.[4,8] In the semi-empirical models, the decay portion of the pressure history at the thrust wall was not analyzed in detail, although the plateau was analyzed. And the one-γ model was adopted in the semi-empirical models, whereas the two-γ model was adopted in this work. To formulate the impulse per unit cross section per one cycle of a simplified PDE, one has to integrate the pressure history at the thrust wall with respect to time. In the semi-empirical models, the impulse per unit cross section per one cycle contributed by positive overpressure $I_{\text{cyc}(+)}$ was given by a semi-empirical formula:

$$I_{\text{cyc}(+)} = K(p_3 - p_1)t_{\text{CJ}} \tag{42}$$

where $K \approx 5.4$ and 4.8 were recommended in Refs. 4 and 8, respectively. In this work, $I_{\text{cyc}(+)}$ was given by Eq. (38), and accordingly, K is expressed as

$$K = K(\gamma_1, \gamma_2, M_{\text{CJ}}) = \delta_B + F_{n'}(\delta_{A1}, \delta_{A2}) \tag{43}$$

That is, the parameter K is not a constant but a function of γ_1, γ_2, and M_{CJ} in this work, and the behavior of it was shown in Fig. 8. From Fig. 8, $K \approx 4$ for typical CJ Mach numbers: $M_{\text{CJ}} \approx 5 \sim 7$. This is a little smaller than the recommended values in Refs. 4 and/or 8. However, the following should be noted. The two-γ model was adopted in this work, whereas the one-γ model was adopted in Refs. 4 and 8. As mentioned earlier, the one-γ model would bring the plateau

pressure in the thrust history p_3 smaller by a factor of γ_2/γ_1 than the two-γ model when $M_{CJ}^2 \gg 1$, which is almost satisfied in most laboratory experiments. As shown in Table 3, $\gamma_2/\gamma_1 \approx 0.81 \sim 0.87$ typically. Therefore, both this work and the semi-empirical models predict similar values of I_{cyc}, I_{sp}, and I_{spf} for current laboratory experiments.

This work has two significant aspects compared with the semi-empirical models previously proposed.[4,8] First, the results of this work can be used for the cases of smaller M_{CJ} than current laboratory experiments in principle because this work needs no empirical parameter that has to be determined by using the results of current laboratory experiments. Second, this work can predict the duration during which overpressure at the thrust wall is positive, namely, $t_{exhaust}$. This duration is very important when we determine the time sequence of the valves in a PDE.

Conclusions

We analytically formulated the pressure history at the thrust wall of a simplified pulse detonation engine without any empirical parameters by using some appropriate approximations. The validity of the approximations we used was examined by using numerical simulations. The derived formulas were validated by comparing them with numerical and experimental results in the parameter range of $4.9 < M_{CJ} < 7.3$. On the pressure history at the thrust wall, the derived formulas reproduced the numerical and experimental results very well as a whole although the derived formula for the decay portion predicted a little lower pressure. On the specific impulse, the derived formulas reproduced the numerical and experimental results within better than 5% except for the case of $C_2H_2+2.5O_2$. Because the derived formulas are valid in the parameter range of $1 < M_{CJ} < 5.5$ from the gas-dynamic consideration, we conclude that the derived formulas are valid in the parameter range of $1 < M_{CJ} < 7.3$. The validity of the derived formulas in the parameter range of $7.3 < M_{CJ}$ needs further examination.

Acknowledgments

The organization of this joint research was supported by Hokkaido Technology Licensing Office Co., Ltd. This work was financially supported by Regional Research and Development Consortium Project from Hokkaido Bureau of Economy, Trade and Industry. We sincerely thank Katsumi Tanaka, National Institute of Advanced Industrial Science and Technology, Japan, for his valuable advice on the specific-heat ratio of the burned gas.

References

[1]Kailasanath, K., "Review of Propulsion Applications of Detonation Waves," *AIAA Journal*, Vol. 38, No. 9, 2000, pp. 1698–1708.

[2]Nicholls, J. A., Wilkinson, H. R., and Morrison, R. B., "Intermittent Detonation as a Thrust-Producing Mechanism," *Jet Propulsion*, Vol. 27, No. 5, 1957, pp. 534–541.

[3]Zhdan, S. A., Mitrofanov, V. V., and Sychev, A. I., "Reactive Impulse from the Explosion of a Gas Mixture in a Semiinfinite Space," *Combustion, Explosion, and Shock Waves*, Vol. 30, No. 5, 1994, pp. 657–663.

[4]Zitoun, R., and Desbordes, D., "Propulsive Performances of Pulsed Detonations," *Combustion Science and Technology*, Vol. 144, 1999, pp. 93–114.

[5]Schauer, F., Stutrud, J., and Bradley, R., "Detonation Initiation Studies and Performance Results for Pulsed Detonation Engine Applications," AIAA Paper 2001-1129, Jan. 2001.

[6]Wintenberger, E., Austin, J. M., Cooper, M., Jackson, S., and Shepherd, J. E., "Impulse of a Single-Pulse Detonation Tube," California Inst. of Technology, Graduate Aeronautical Labs., GALCIT Rept. FM00-8, Pasadena, CA, Aug. 2002.

[7]Cooper, M., Jackson, S., Austin, J., Wintenberger, E., and Shepherd, J. E., "Direct Experimental Impulse Measurements for Detonations and Deflagrations," *Journal of Propulsion and Power*, Vol. 18, No. 5, 2002, pp. 1033–1041.

[8]Wintenberger, E., Austin, J. M., Cooper, M., Jackson, S., and Shepherd, J. E., "Analytical Model for the Impulse of Single-Cycle Pulse Detonation Tube," *Journal of Propulsion and Power*, Vol. 19, No. 1, 2003, pp. 22–38.

[9]Endo, T., and Fujiwara, T., "A Simplified Analysis on a Pulse Detonation Engine Model," *Transactions of the Japan Society for Aeronautical and Space Sciences*, Vol. 44, Feb. 2002, pp. 217–222.

[10]Landau, L. D., and Lifshitz, E. M., "The Propagation of a Detonation Wave," *Fluid Mechanics*, 2nd ed., Butterworth-Heinemann, Oxford, 1987, Sec. 130.

[11]Landau, L. D., and Lifshitz, E. M., "Detonation," *Fluid Mechanics*, 2nd ed., Butterworth-Heinemann, Oxford, 1987, Sec. 129.

[12]Landau, L. D., and Lifshitz, E. M., "One-Dimensional Similarity Flow," *Fluid Mechanics*, 2nd ed., Butterworth-Heinemann, Oxford, 1987, Sec. 99.

[13]Landau, L. D., and Lifshitz, E. M., "Arbitrary One-Dimensional Gas Flow," *Fluid Mechanics*, 2nd ed., Butterworth-Heinemann, Oxford, 1987, Sec. 105.

[14]Reynolds, W. C., "The Element Potential Method for Chemical Equilibrium Analysis: Implementation in the Interactive Program STANJAN, Version 3," Dept. of Mechanical Engineering, Stanford Univ., TR A-3991, Stanford, CA, Jan. 1986.

[15]Matsuo, A., Fujii, K., and Fujiwara, T., "Flow Features of Shock-Induced Combustion Around Projectile Traveling at Hypervelocities," *AIAA Journal*, Vol. 33, No. 6, 1995, pp. 1056–1063.

[16]Wilson, G. J., and MacCormack, R. W., "Modeling Supersonic Combustion Using a Fully Implicit Numerical Method," AIAA Paper 90-2307, July 1990.

A. Karagozian
Associate Editor